CHALMERS
UNIVERSITY OF TECHNOLOGY

Telecommunication Compatibility Evaluation for Co-existing Quantum Key Distribution in Homogenous Multicore Fiber

Citation for the original published paper (version of record):
Lin, R., Udalcovs, A., Ozolins, O. et al (2020). Telecommunication Compatibility Evaluation for Co-existing Quantum Key Distribution in
Homogenous Multicore Fiber. IEEE Access, 8: 78836-78846.
http://dx.doi.org/10.1109/ACCESS.2020.2990186

(article starts on next page)

IEEE Access
Multidisciplinary | Rapid Review | Open Access Journal

Received March 27, 2020, accepted April 20, 2020, date of publication April 24, 2020, date of current version May 11, 2020.

Digital Object Identifier 10.1109/ACCESS.2020.2990186

Telecommunication Compatibility Evaluation for Co-existing Quantum Key Distribution in Homogenous Multicore Fiber

RUI LIN[1], (Member, IEEE), ALEKSEJS UDALCOVS[2], (Member, IEEE), OSKARS OZOLINS[2,3], (Member, IEEE), XIAODAN PANG[3], (Senior Member, IEEE), LIN GAN[4], MING TANG[4], (Senior Member, IEEE), SONGNIAN FU[4], (Senior Member, IEEE), SERGEI POPOV[3], THIAGO FERREIRA DA SILVA[5], GUILHERME B. XAVIER[6], AND JIAJIA CHEN[1], (Senior Member, IEEE)

[1]Department of Electrical Engineering, Chalmers University of Technology, 41296 Gothenburg, Sweden
[2]RISE Research Institutes of Sweden AB, Kista 16440, Sweden
[3]KTH Royal Institute of Technology, Kista 16440, Sweden
[4]School of Optical and Electronic Information, Huazhong University of Science and Technology, Wuhan 430074, China
[5]Optical Metrology Division, National Institute of Metrology, Quality and Technology, Duque de Caxias 25250-020, Brazil
[6]Institutionen för Systemteknik, Linköpings Universitet, 58183 Linköping, Sweden

Corresponding author: Jiajia Chen (jiajiac@chalmers.se)

This work was supported in part by the Ceniit–Linköping University, Swedish Research Council, in part by the Swedish Foundation for Strategic Research (SSF), in part by the Göran Gustafsson Foundation, in part by the Celtic-Plus sub-project SENDATE-EXTEND funded by Vinnova, in part by the EU H2020 project TWILIGHT under Grant 871741, in part by the Vinnova funded project Centre for Software-Defined Optical Networks, in part by the National Natural Science Foundation of China under Grant 61722108, in part by the H2020 NEWMAN Project under Grant 752826, and in part by AoA ICT seed project and Genie project funded by Chalmers University of Technology Foundation. The Knut and Alice Wallenberg foundation is acknowledged for equipment funding and Tektronix for equipment loan.

ABSTRACT Quantum key distribution (QKD) is regarded as an alternative to traditional cryptography methods for securing data communication by quantum mechanics rather than computational complexity. Towards the massive deployment of QKD, embedding it with the telecommunication system is crucially important. Homogenous optical multi-core fibers (MCFs) compatible with spatial division multiplexing (SDM) are essential components for the next-generation optical communication infrastructure, which provides a big potential for co-existence of optical telecommunication systems and QKD. However, the QKD channel is extremely vulnerable due to the fact that the quantum states can be annihilated by noise during signal propagation. Thus, investigation of telecom compatibility for QKD co-existing with high-speed classical communication in SDM transmission media is needed. In this paper, we present analytical models of the noise sources in QKD links over heterogeneous MCFs. Spontaneous Raman scattering and inter-core crosstalk are experimentally characterized over spans of MCFs with different refractive index profiles, emulating shared telecom traffic conditions. Lower bounds for the secret key rates and quantum bit error rate (QBER) due to different core/wavelength allocation are obtained to validate intra- and inter-core co-existence of QKD and classical telecommunication.

INDEX TERMS Quantum key distribution, spatial division multiplexing, telecommunications, communication system security.

I. INTRODUCTION

Over previous years, data traffic has been continuously experiencing an exponential growth across the globe [1]. As one of the key supporting techniques supplying enormous data traffic, optical communication has been focused on finding innovative ways in order to unblock the potential transmission bandwidth. However, fiber-optic networks are vulnerable to eavesdropping. An eavesdropper with physical access to fiber can retrieve a portion of the propagating signals just by bending the fiber without being noticed [2]; depending on the type of encryption, the data can be decrypted in principle

The associate editor coordinating the review of this manuscript and approving it for publication was Jesús Hamilton Ortiz.

by one eavesdropper equipped with a quantum computer, without resorting to brute-force attacks. Quantum key distribution (QKD), also known as quantum cryptography [3], [4] has the potential to address this great security concern by exploiting quantum physics principles. In a QKD system, the secret keys are transmitted between the pair of sender and receiver, Alice and Bob, in the form of quantum states which are unclonable, showing that QKD is a promising technique for cyber security. Since the first QKD protocol BB84 [5], significant efforts have been made to develop security proofs and experimental demonstrations. By now, there are not only lab-based demonstrations, but also real-world use cases have been reported in installed fiber infrastructure [6], [7], free-space links [8], [9] and satellite links [10]. Dynamic end-to-end key exchange was also recently demonstrated in a QKD secured network [11], showing its potential to secure the future communication networks [12].

In a QKD system, information can be either encoded in the polarization or phase of single-photon states, namely, discrete-variable QKD (DV-QKD), or in the quadrature of the quantized electromagnetic field, namely continuous variable (CV-QKD). DV-QKD has morecomplete security proof, while CV-QKD can be implemented by using mature telecom equipment [13]. In addition, compared to CV-QKD, DV-QKD is able to reach much longer transmission distances. In practical implementation, extremely faint optical pulses are required to be handled by a distant pair of clients regardless which type of QKD system is deployed. Considering the high cost of fiber deployment, coexistence of quantum and high-speed data channels in the same fiber is highly desirable. However, classical communication over a shared optical network infrastructure tends to create noise into the quantum channel, jeopardizing the QKD system performance or even leading to its outage.

QKD signals and classical signals can co-exist in wavelength division multiplexing (WDM) architecture [14]–[19]. They can be allocated either in different bands [14], [17], [18], or together in the C-band [14], [15], [18], [19]. Among those band allocations, the C-band is beneficial [19] for both QKD (in terms of low loss and, thus, longer transmission distance and higher key rate), and the classical data channels, taking advantage from mature transponders and devices. However, the dense wavelength allocation either limits the injection power of the classical channel to a low level [16], which might affect the communication performance of the high-speed data transmission; or requires sophisticated phase filtering techniques rather than commercial devices [14]. Moreover, due to the wavelength dependence of the channel noise, complex channel resource allocation algorithms might be needed in a dynamic scenario to allow the successful secret key distribution [6].

Spatial division multiplexing (SDM) uses the multiplicity of space channels to increase capacity for optical communications and to keep up with the enormous traffic demand [1]. SDM transmission media, represented by multicore fiber (MCF), along with higher capacity for data communication [21]–[23], also provides natural isolation between the adjacent spatial channels. It provides a good alternative for the compatibility of QKD with high-speed classical communication, allowing for higher aggregated key rate and co-existence capacity. Moreover, colorless transceivers for telecommunication can be used in SDM to eliminate the need for WDM transceivers regardless of protocols being used. The first realization of QKD and classical data channels over SDM system was reported in [24]. In a 7-core MCF, 5 of the outer cores are assigned with 10-Gbps signals on the same wavelength while the center core is dedicated to the quantum channel. The 5 nm spectrum spacing is reserved as a guard band between data channel and quantum channel and no detrimental effect on the QKD performance was observed. Recently reported in [25], 370 Gbps aggregated classical data co-existing with 65 Mbps aggregated secret key was realized by parallel transmission over a 7.9 km long, 37-core heterogeneous MCF. Practical fabrication of such a heterogenous MCF is much more difficult than homogeneous MCF, since different cores have distinct configuration parameters. It is also reported that when the quantum channel uses a dedicated core of MCF, network operators can avoid the noise generated by inter-core crosstalk by assigning the wavelengths lying in the guard-band between the classical data channels to the quantum signals [26]. This wavelength allocation strategy can be used to solve the problem of multiplexing of quantum and classical channels and avoids introducing new components for the classical communication channels. More details on experiments merging SDM and QKD can be found in [27].

A theoretical model of QKD over MCF links was reported in [28], mainly focusing on the inter-spatial channel noise. However, the intra-spatial channel noise (in particular with wavelengths carrying high-speed data rather than just a single quantum channel are assigned in the same core) was not investigated yet. In this paper, based on the experimental characterization in [29], we 1) report the analytical models of the two main noise sources in MCF fibers for QKD, i.e., inter-core crosstalk (XT) and intra-core spotaneous Raman scattering (SRS); and 2) provide a lower-bound estimation for the QKD link performance over two types of SDM fibers, considering both intra- and inter-core coexistence with high-speed data channels.

II. SDM TRANSMISSION MEDIA

To be more attractive than parallel single mode fiber (SMF), the lower skew (the spread of propagation delays) among different spatial channels in SDM fiber can be exploited for greater efficiency from hardware sharing to joint processing [30]. Intensive research activities on SDM technologies have been initiated to support Peta (10^{15}) bps data transmission per fiber [31]. The potential technological SDM approaches are ultimately defined by fiber designs. A spatial element in SDM fiber can be a core, a mode, and their combination. For the early stage adoption of SDM fibers, uncoupled or weakly coupled homogeneous single-mode fibers are

TABLE 1. Parameters of two types of MCFs.

	TA-MCF	NT-MCF
Core diameter	8.7 μm	8.7 μm
Core pitch	41.1 μm	41.1 μm
Trench diameter	13.5 μm	-
Cladding diameter	150 μm	150 μm
RI* of each core	1.4639	1.4639
RI of cladding	1.4591	1.4591
RI of the trench	1.4496	-
Attenuation	0.2 dB/km/core	0.2 dB/km/core
Chromatic dispersion	16 ps/nm/km	16 ps/nm/km

*RI: refractive index

practical options thanks to their compatibility with the current infrastructure and ease of fabrication. In this paper, we consider homogenous MCF, where each core is single-mode and has the same configuration parameters. In principle, each of the fiber cores in MCF can act as a separate waveguide so that light can independently propagate through those cores. However, there can be some mode coupling between the cores if the distance between adjacent cores are too small so that the corresponding mode fields have a significant spatial overlap. By giving an extra trench around the normal step index core, strong mode confinement can be realized. Therefore, coupling effect and inter-core XT can be suppressed. Separated by the trench in the refractive index profiles, MCF can be categorized as trench-assisted (TA-MCF) and untrenched MCF (UT-MCF). In this work, we use a span of 2.5 km 7-core TA-MCF and UT-MCF fabricated by the same manufacturer, to analyze the system performance in terms of QKD co-existing with classical communication. The fiber cross-section has one central core and the other six cores aligned in a hexagonal pattern. The parameters of the MCFs considered in this paper are listed in TABLE 1.

III. METHODOLOGY

We investigate the telecom compatibility of QKD classical transmission over MCFs by:

1) First, recording the photon leakage coming from the classical channels located at different wavelengths and/or cores into the quantum channel;
2) Adding the measured photon leakage to the total noise of a QKD system (using [32] as the theoretical model and detection parameters from [33] for a reference system as a benchmark), and, then, calculating the lower bound for the secret key rate (SKR) shared between the sender (Alice) and receiver (Bob) after the post-processing; and
3) Finally estimating the SKR and quantum bit error rate (QBER) as a function of transmission distance, taking into account the characterized noise.

A. QKD SYSTEM MODEL

A basic QKD system consists of the source, channel and detector [32]. The overall transmittance η, describing the ratio of the photons transmitted by Alice and successfully detected by Bob, can be written as:

$$\eta = t_{AB}\eta_{Bob}, \tag{1}$$

where t_{AB} is the channel transmittance and η_{Bob} is the efficiency of Bob's receiver. The latter can be expressed as the product of transmittance of optical components, t_{Bob}, and the single-photon detector efficiency, η_{det}, i.e.,

$$\eta_{Bob} = t_{Bob}\eta_{det}. \tag{2}$$

For a fiber based QKD system, the channel transmittance is mainly determined by the loss, expressed as:

$$t_{AB} = 10^{-\alpha L/10}, \tag{3}$$

where α denotes the attenuation in dB per unit of length, and L is the fiber transmission distance. Note, that in practical systems coupling loss due to connectors/splices should also be included in $\boldsymbol{t_{AB}}$.

B. SECRET KEY RATE AND QBER

Considering the infinite decoy states technique [33] applied, the SKR can be expressed as:

$$SKR \geq Q_1\left[1 - H_2\left(e_1\right)\right] - Qf\left(E\right)H_2\left(E\right), \tag{4}$$

where Q_1 is the probability of a single-photon pulse sent by Alice and being detected by Bob, e_1 is the error probability for the single-photon state, Q is the probability of the detection by Bob for all-photon states sent by Alice. $H_2()$ is the Shannon binary entropy function, and $f()$ is the error correction inefficiency factor function. E represents the total QBER, which can be calculated as

$$E = \frac{1}{Q}\left[\frac{1}{2}Y_0 + \gamma\left(1 - e^{-\mu\eta}\right)\right], \tag{5}$$

where $1/2Y_0$ is the system noise in a QKD system using BB84 protocol [5] (probability of detection by Bob in wrong detector when no photon is sent by Alice), γ depicts the alignment error of the optical system, and μ is the average photon flux set by Alice for signal states.

Targeting a better utilization of fiber efficiency, the co-existing of classical signal and quantum signal over the same transmission media is considered. The system noise contributes to Q, Q_1, E and e_1, and consists of the total photon leakage from classical signal into the quantum channel due to inter-core XT and intra-core SRS, as well as the (average) dark count probability of the single-photon detectors (SPD). Assuming that a dedicated wavelength is assigned for the quantum channel regardless of spatial allocation, inter-core XT is out-of-band noise, which can be mitigated by pre-filtering the unwanted ASE noise for the quantum channel at the transmitter side and by cascading bandpass filters at the receiver side. The SRS, which depends on spectral distance, may not be neglectable in the case that the same core is populated by both quantum and classical communication. The inelastic scattering of the photons from classical channel results in the in-band noise affecting the key delivery. A high level of photon contamination eventually saturates

the SPD. In this paper, the total noise count rates, including the dark count rate, are obtained through experimental characterization. The SPD for counting the photon rate at the quantum channel works in gated mode with 1 MHz repetition rate, 10 μs deadtime, 10% overall detection efficiency, and 1 ns wide effective gate width. Dark count probability is 1.3×10^{-5} per gate.

In the following sections, the noise models for both intra-core and inter-core co-existence in homogenous MCF, as well as the SKR and QBER performance simulation will be presented. The detection parameters from [33] are used for the QKD performance evaluation, including the efficiency of Bob's receiver $\eta_{Bob} = 0.045$, detection efficiency $\eta_{det} = 0.1$, and the alignment of the optical system $\gamma = 0.033$. The GYS experiment has been widely used for many years as a benchmark in theoretical analyses of secret key rates with different models, and therefore are used to make our results comparable with other relevant works. An infinite-decoy-state QKD method is simulated with an optimized average photon flux $\mu = 0.48$ and error correction inefficiency factor $f(E) = 1.22$.

IV. INTRA-CORE CO-EXISTENCE

A. SRS NOISE MODEL

Photon-photon interaction causes both Brillouin scattering and Raman scattering, potentially resulting in frequency-shifted photons from the classical signal to the quantum channel band. The wavelength shift due to Brillouin scattering is within 10 GHz from the initial wavelength and, therefore, can be filtered as out-of-band noise for the QKD allocated in the adjacent spectral channel which is at least tens of GHz away (50/100 GHz channel spacing for dense WDM). The Raman scattering, on the contrary, leads to photon generation in a much wider band at wavelengths longer (Stokes) or shorter (anti-Stokes) than the initial wavelength [34]. The Raman scattering can shift from the data channel covering the entire C-band [34] and leaving in-band noise for the QKD channel.

The in-band noise (per detection temporal gate width) generated by SRS from the data channel can be written, in the co-propagating case, as:

$$P_{SRS\_co} = P_{out}(L)\beta(\lambda) \cdot \Delta, \tag{6}$$

where P_{out} is the power of the laser at the fiber output, L is the fiber length, $\beta(\lambda)$ is the wavelength-dependent SRS coefficient, and $\Delta\lambda$ is the wavelength channel bandwidth. P_{out} can be expressed as:

$$P_{out}(L) = P_{in}e^{-\alpha L}, \tag{7}$$

where $\boldsymbol{P_{in}}$ is the input power to the fiber. When several data channels are propagating simultaneously, the in-band noise for the quantum channel can be obtained by the incoherent sum of the contribution from each single data channel with corresponding SRS coefficient $\boldsymbol{\beta}(\boldsymbol{\lambda})$ [34], [35].

B. CHARACTERIZATION

Wavelength dependence of SRS is measured by injecting an optical signal at different wavelengths and measuring the count rate induced in the quantum channel. As shown in Fig. 1, we first use a tunable continuous wave (CW) distributed feedback (DFB) laser covering a tuning range in the C-band. At the transmitter side, pre-filtering is done by cascading a waveshaper [36] together with a fiber Bragg grating (FBG) in reflective mode centered at the quantum channel wavelength form a spectrum notch mitigating the ASE noise at the quantum channel. An isolator between them is used to prevent the reflective light from FBG1 damaging the waveshaper. Then the CW is injected in one of the cores (core 7) in the MCF through the fan-in module. After the fiber span, two WDMs and FBG2 (centered at the quantum channel) are employed to further eliminate out-of-band noise effects. The FBGs are 100 GHz full-width half-maximum (FWHM). A single photon detector (SPD) (IdQuantique id 210), working in gated mode with 1 MHz repetition rate, 10 μs deadtime, 10% overall detection efficiency, and 1 ns wide effective gate width is used for counting the photon rate left at the quantum channel. Dark count probability is 1.3×10^{-5} per gate. The photon count rate at each wavelength is first measured, subtracted by the dark account and then normalized by the detection efficiency.At the receiver end, an optical power meter (PM) is used for power monitoring.

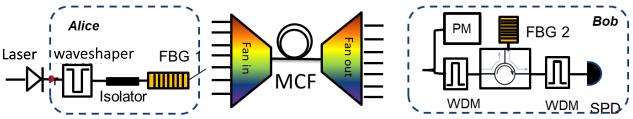

FIGURE 1. SRS coefficient and inter-core XT measurement setup. FBG: fiber Bragg grating; PM: optical power meter; WDM: wavelength multiplexer; SPD: single-photon detector.

Note that power attenuation is caused not only by the optical fiber itself, but also the coupling and fan- in/fan-out modules, which can be calibrated by comparing the theoretical and measured noise level. In the link performance simulation, the effects of constant loss of coupling and fan-in/fan-out modules are mitigated.

In intra-core SRS coefficient characterization, wavelength 1546.92 nm is set as the quantum channel. We first scan the wavelengths and monitor the photon detection without MCF insertion. After normalization by the detection efficiency, the core-by-core photon count dependence on wavelength is shown in Fig. 2. Stokes and anti-stokes shift can be clearly observed in both of MCFs. Comparing to the TA-MCF, there exists higher average SRS noise along the C-band and more fluctuation among different cores in UT-MCF. Then the launch power is scanned from -0.5 dBm to -8.5 dBm, the photon detection behavior in the center core of both MCFs can be seen in Fig. 3. The frequency dependence of photon detection has an approximate linear behavior on both sides of the quantum channel. After averaging all the cores, the linear

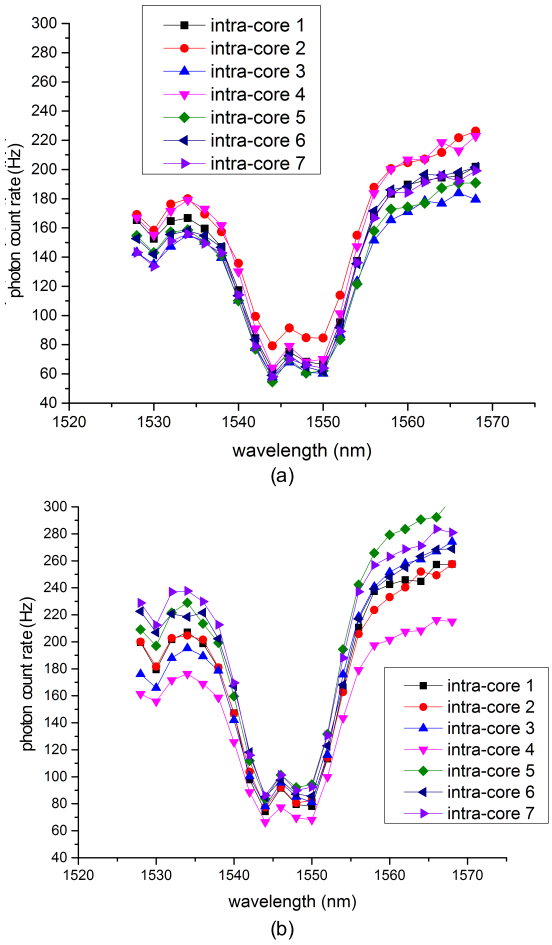

FIGURE 2. SRS coefficient measurement in (a) TA-MCF and (b) UT-MCF with injection power of −0.5 dBm.

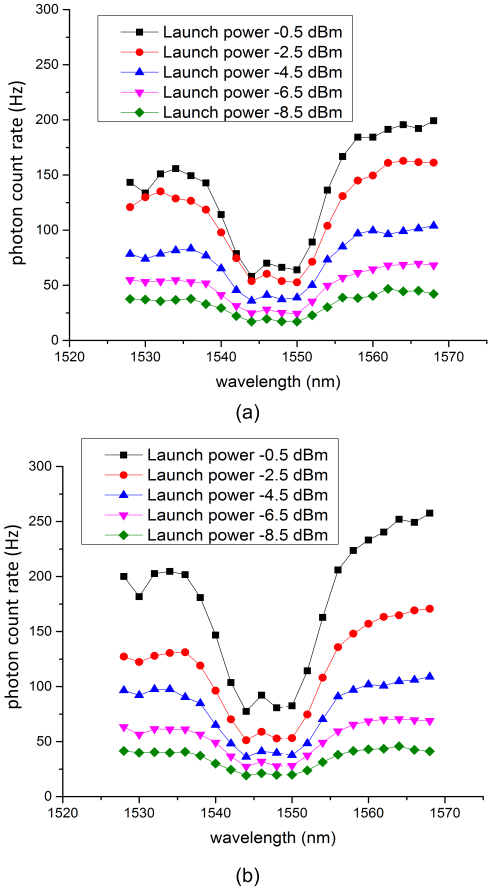

FIGURE 3. Injected power scanning in core 7 for SRS coefficient measurement in (a) TA-MCF and (b) UT-MCF.

fitting results of the SRS co-efficiency of two types of MCFs are listed in Table 2.

TABLE 2. SRS efficiency of both types of MCFs after averaging in all cores, in unit ($km{\cdot}nm^{-1}$).

	$\lambda < \lambda_q$	$\lambda > \lambda_q$
TA-MCF	11.968±**0.863**	6.06±**0.40**
UT-MCF	16.3±**1.2**	7.13±**1.03**

C. PERFORMANCE EVALUATION

Based on the noise characterization obtained in the previous section, we assess the impact on the quantum link in both types of MCFs. Using (1)-(5), the QBER and SKR are estimated based on the SRS noise contribution when the data channel and quantum channel are allocated in the same core. In both Stokes and anti-Stokes shift ranges, wavelengths in high and low SRS windows are picked to show the impact on the quantum channel, i.e., 1528 nm and 1544 nm represent high and low SRS window in Stokes range, while 1548 nm and 1558 nm represent high and low SRS windows among anti-Stokes shift, respectively. In Fig.4, we can see the SKR and QBER as a function of transmission distance with the input power of the data channel set as –0.5 dBm. The black solid curve shows the benchmark, where an SMF is dedicated for the quantum channel, with no shared classical signals [33]. In this case only the link attenuation contributes to the quantum performance along the signal propagation. It is clearly observed that there is a serious performance degradation even when the wavelength in the low SRS window is assigned for the data signal. In contrast to UT-MCF, the lower SRS co-efficiency in TA-MCF enables a slight improvement of the QBER and SKR. Note that QBERs below the 11% limit are obtained in all cases where a positive SKR can be achieved, indicating that error correction and privacy amplification allows the generation of a shared secret key [37].

In intra-core SRS measurement, FBGs, waveshaper, and WDMs are cascaded to provide isolation as high as ∼100 dB for the quantum channels, inducing negligible crosstalk when no fiber link is present. It, therefore, shows how many in-band photons are generated on the quantum channel when the data signal and quantum signal are located in the same spatial channel.

It is worth to notice that SKR performance varies if using SPDs with different detection gate widths, repetition rates,

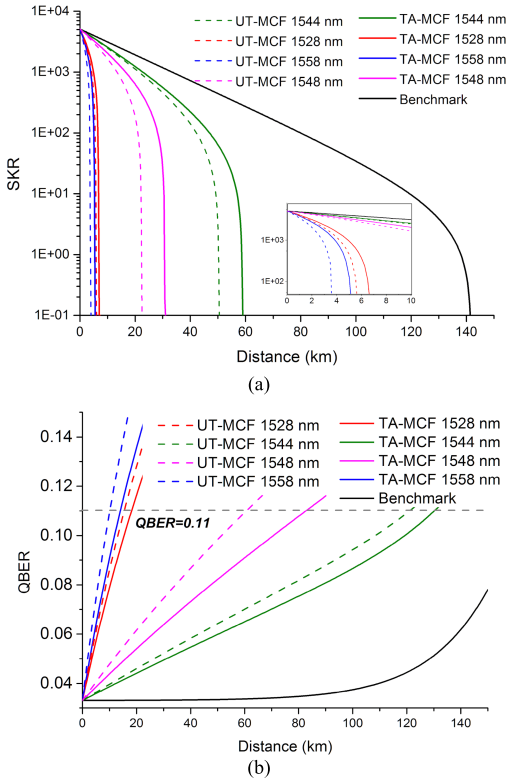

FIGURE 4. Simulated (a) Secret key rate and (b) QBER as a function of fiber transmission distance. Solid curves: TA-MCF; dashed curves: UT-MCF, black curves: SMF as benchmark.

dark count and detection efficiency [38]. However, a relative relationship among the cases adopting different types of MCFs with different channel allocation would not be much influenced.

V. INTER-CORE CO-EXISTENCE

MCF provides the possibility to co-existing quantum and data communication in different spatial channels in a single fiber. In contrast to the intra-core co-existence, refractive index gaps between adjacent cores contribute to the noise isolation, so that the filtering requirement in quantum channel can be relaxed. In this section, the quantum channel performance is assessed with the presence of high-speed data communication in different cores.

A. NOISE MODEL

We consider the high-speed data channel operating on wavelength λ, which is coupled to the quantum channel on the same wavelength in adjacent cores. Furthermore, both the high-speed data signal and quantum power attenuate with fiber distance, according to (7). In the case where an individual core is assigned for the quantum channel, an inter-core XT is the main contributor for the noise measurement.

The inter-core XT coupling to the neighboring core can be expressed as a function of fiber length L:

$$P_{XT}(L) = P_{signal}(L)\, XT_{index} L, \tag{8}$$

where $P_{signal}(L)$ is the high-speed data signal power, and XT_{index} is the crosstalk coefficient between the neighboring cores. The noise photons count due to inter-core XT is obtained as:

$$XT_{nr}(L) = P_{XT}(L) / (hc/\lambda), \tag{9}$$

where h denotes the Planck's constant, and c is the speed of light in the fiber.

B. NOISE CHARACTERIZATION

We experimentally characterize the penalty for a QKD link over both TA- and UT-MCFs with the presence of beyond 100 Gbps classical communication signals per wavelength used for high-speed data transmission [29].

The setup is similar to that shown in Fig.1. A tunable DFB laser operating at the C-band is used for the data channel transmitter (Tx). 8 wavelengths (1525 nm to 1565 nm except 1550 nm, with interval of 5 nm) are swept in the C-band to investigate the impact of the wavelength dependence on the quantum channel. A 56 GBaud, 4-level pulse amplitude modulation (PAM4) signal is generated with a digital-to-analog convertor (DAC, Anritsu G0374), and amplified to drive a linearly biased Mach-Zehnder modulator (MZM). The output optical signal is amplified by an Erbium-doped fiber amplifier (EDFA) and filtered by a tunable band-pass filter (BPF) of 100 GHz 3 dB bandwidth with ~30 dB rejection ratio. A variable optical attenuator (VOA) is used to adjust the launched power. The optical signal is power split, temporally de-correlated and coupled into the MCF under test via a fan-in module. After propagation, the spatial channels are de-multiplexed by a fan-out module so that the signals from each core are connected to a SMF. The high-speed data channel is detected by a receiver consisting of a pre-amplifier, a BPF and a photodetector (3 dB bandwidth of ~33 GHz), before being sampled at a digital storage oscilloscope (DSO) and demodulated off-line. A decision-feedback equalizer with 43-feed-forward taps and 12-feedback taps is used for channel equalization.

For receiving the quantum channel, the center core's output is reflected by a FBG centered at 1550 nm before passing through a BPF to filter the out-of-band photons. The FBGs and BPF used in this measurement can only provide ~ 66 dB isolation, which is not as good as that in intra-core experimental setup (i.e., ~100dB in the intra-core co-existence experiment above). On top of the isolation provided by the out-of-band noise filtering, the measured inter-core XT for the 2.5 km UT-MCF is about −45 dB, while for the 2.5 km TA-MCF is about −65 dB. The SPD for counting the photon rate at the quantum channel works in a gated mode with 1 MHz repetition rate, 10 μs deadtime, 10% overall detection efficiency, and 1 ns wide effective gate width. The dark count probability is 1.3×10^{-5} per gate. The quantum channel set in the center core represents the worst spatial case in terms of inter-core XT when the other cores are occupied by high-speed data. The inter-core photon contamination includes out-of-band noise, i.e., the inter-core XT, and

in-band noise, i.e, the XT-induced SRS. Two distinct layouts are used in the measurements:

1) Side-core configuration, where only the side cores were assigned for high-speed data communication. In this case, the XT-induced SRS is negligible and the noise detection is dominated by the inter-core XT.

2) All-core configuration, where measurements were also performed for the case when the center core was also used for the data channel, in addition to the side cores. In this configuration, the photon count rate detection at the quantum channel takes into account both inter-core XT and SRS noise originated by the classical channel in the same core.

The detection of leaked photons to the quantum channel due to simultaneous data transmission are measured in both side-core and all-core configurations. In Fig. 5, wavelengths 1530 nm, 1540 nm and 1560 nm are selected to show the wavelength dependence.

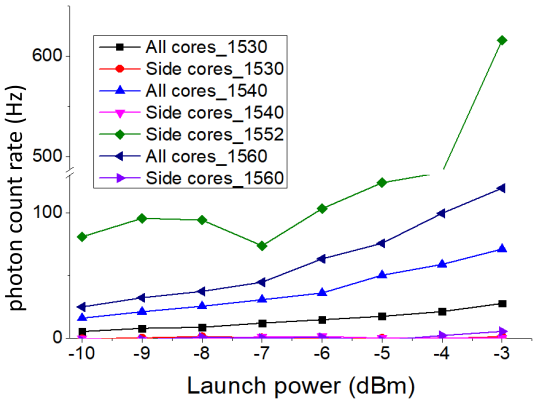

FIGURE 5. Photon count rate of the quantum channel in UT-MCF as a function of launch power with different wavelengths assigned to data transmission for side-core and all-core configurations. The noise contribution in all-core configuration originated from both inter-core XT and SRS. The high photon count rate at 1552 nm is due to the filtering profile leakage close to the quantum channel.

The measurement results when data signals carried by wavelengths 1530 nm, 1540 nm, 1552 nm and 1560 nm in the UT-MCF are shown in Fig.5. In the side-core configuration, photon detection at the quantum channel, i.e., 1550 nm in the central core, is very close to the dark count limit at $\sim 1.3 \times 10^{-5}$ per gate when the wavelengths assigned to data transmission are away from the quantum channel, represented by red, rose and purple curves in Fig. 5. When the center core is also assigned to high-speed data transmission, photon contamination sharply increases. The photon detection rates in the quantum channel are less than 100 Hz given that the launch power of the data channel is lower than -4 dBm. Once the wavelength close to the quantum channel is used for carrying high-speed data, i.e., 1552 nm in Fig. 5, a remarkable increase of the photon detection can be observed, even when the center core is free of classical data. Since no obvious wavelength dependence in the rest of the C-band can be observed, we attribute the higher detection rate at 1552 nm to limitations in the spectrum profile of the FBGs. The TA-MCF in side-core configuration was also measured. It performs very similar as UT-MCF and, therefore, is not displayed in Fig. 5. Using 1552 nm to deliver high-speed data in all the side cores, a considerable increase in the detection rate can be observed. For classical communication over the other wavelengths, even at the maximum launch power (-3 dBm), the photon detection is very close to the SPD's dark limit. Compared to UT-MCF, an obviously lower inter-core XT in TA-MCF results in the smaller number of photons passing through the detection filter, i.e., the FBG and the BPF. To visualize the small difference between the photon detection after transmission over the 2.5 km MCFs, we estimate the SKR performance in the two types of MCFs, which will be shown in the next subsection.

C. PERFORMANCE EVALUATION

Based on the noise characterization, the estimated SKR following the 2.5 km MCF transmission is shown in Fig. 6. for different wavelengths assigned to data transmission for both types of MCFs. The all-wavelength ("All w" in legend) case corresponds to using all 8 measured wavelengths (1525 nm to 1565 nm with interval of 5 nm, except for 1550 nm) for data transmission. Assuming a 1 MHz repetition rate used in the QKD system, ~4.4 kbps SKR can be achieved for both fibers in the side-core configuration. A negligible difference on the SKR can be observed between the deployment of the two types of MCFs, even though a higher inter-core crosstalk is in the UT-MCF. The exception occurs when 1552 nm is used as the data channel (i.e., All w + 1552 nm), and the key generation can only be realized at a considerably lower rate in the UT-MCF compared to that in the TA-MCF. When the center core is additionally employed for data transmission, i.e., all-core configuration, the quantum channel is affected by the inter-wavelength crosstalk, and a penalty on the secret key rate can be seen. We also include the expected SKR for all-core configuration when all 8 measured wavelengths are employed simultaneously, where an obvious penalty on the SKR can be observed in both types of MCFs.

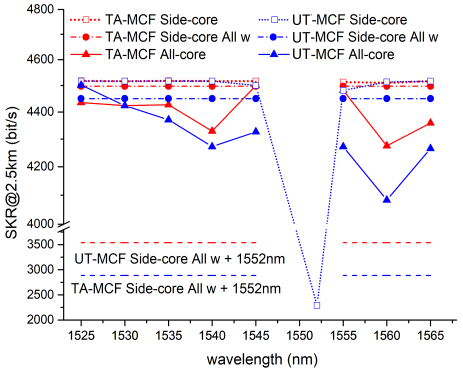

FIGURE 6. Simulated secret key rate at 2.5 km for both of MCFs as a function of the wavelength assigned for data transmission.

In Fig. 7(a), we plot the estimated lower bound of the SKR as a function of transmission distance, taking into account the fiber attenuation of the classical and quantum channels. When a dedicated core and a dedicated wavelength is assigned to

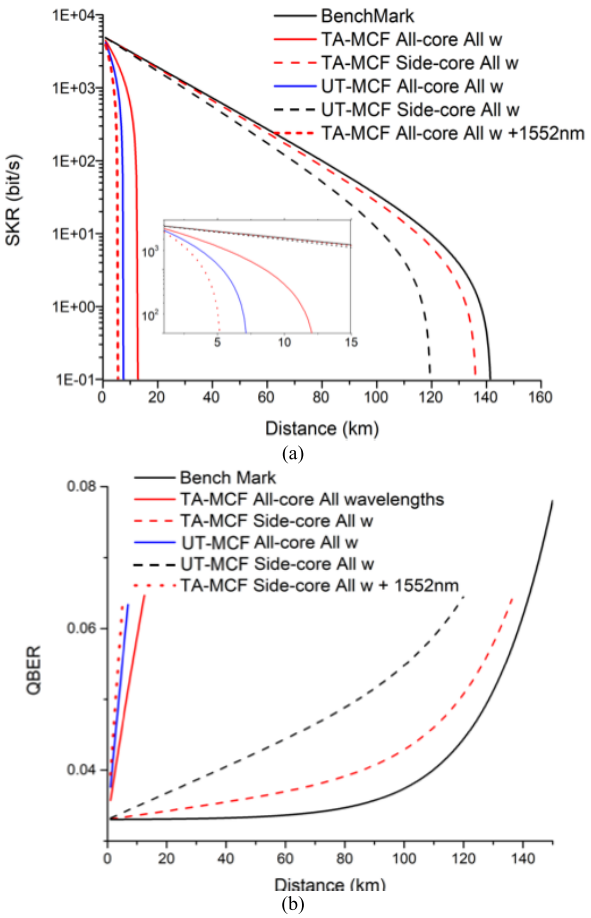

FIGURE 7. (a) Simulated secret key rate as a function of distance both MCFs; and (b) QBER performance for all the configurations within valid transmission distance.

QKD, a small negative effect of the crosstalk on the SKR performance can be observed (see red and blue dashed curves close to the benchmark in black). Very short maximum distance for secure key exchange ($\sim$ 5 km) is observed, if the wavelength close to the quantum channel (i.e., 1552 nm is used in the measurement) is assigned to data delivery in the UT-MCF. In all-core, all-wavelength configuration, both inter- and intra-core coexistence of QKD and classical channels are allowed, causing the SKR to quickly fall down in both types of MCFs (red and blue curves). The red dense dashed curve shows the case where a wavelength close to the QKD channel is carrying classical communication. With insufficient out-of-band filtering, the TA-MCF can only support non-zero SKR within a few kilometers. As shown in Fig. 7(b), QBER below the 11% limit at non-zero SKR in all cases are achieved. A less noisy quantum channel yields better QKD performance, which can be realized by using filters with a higher rejection ratio and limiting the launch power of the classical channels.

VI. CONCLUSION

In this paper, we propose a methodology to evaluate the telecommunication compatibility of QKD in homogenous SDM configuration. The noise model for the QKD co-existence with classical communication in homogenous MCF is presented and the performances of QKD system in UT- and TA-MCFs are evaluated by simulation based on the experimental characterization of co-propagation noise. Moving from SMF to MCF-based co-existing system, significant telecommunication capacity increase can be enabled. Nevertheless, a dedicated core for QKD is preferred due to the extra spatial isolation provided. Reusing the wavelength assigned to quantum channels for telecommunication could stop the key distribution. Even if a wavelength in the low noise window is picked to carry classical signal, a severe performance degradation in terms of the transmission distance and QBER can be found in the QKD due to SRS. Consequently, it is preferable not to transmit classical data in the core containing the quantum signals. In inter-core coexistence case, although avoiding using the wavelength of quantum channel for data transmission, the quantum channel's performance is still affected with slight penalty comparing to the SMF case due to imperfect isolation provided by the refractive index profile in MCF design. A slightly larger penalty in the UT-MCF is observed as expected due to a higher inter-core XT. We have nevertheless shown the telecom compatibility of QKD can be achieved by homogenous SDM approach, provided additional penalties should be taken into account in the system design. For example, the QKD over SDM system performance can be considered for the future work.

REFERENCES

[1] P. J. Winzer, D. T. Neilson, and A. R. Chraplyvy, "Fiber-optic transmission and networking: The previous 20 and the next 20 years [Invited]," *Opt. Express*, vol. 26, no. 18, pp. 24190–24239, Sep. 2018.
[2] N. Skorin-Kapov, M. Furdek, S. Zsigmond, and L. Wosinska, "Physical-layer security in evolving optical networks," *IEEE Commun. Mag.*, vol. 54, no. 8, pp. 110–117, Aug. 2016.
[3] V. Scarani, H. Bechmann-Pasquinucci, N. J. Cerf, M. Dušek, N. Lütkenhaus, and M. Peev, "The security of practical quantum key distribution," *Rev. Mod. Phys.*, vol. 81, no. 3, pp. 1301–1350, 2009.
[4] M. A. Nielsen and I. L. Chuang, *Quantum Computation and Quantum Information*. Cambridge, U.K.: Cambridge Univ. Press, 2000.
[5] C. H. Bennett and G. Brassard, "Quantum cryptography: Public key distribution and coin tossing," in *Proc. Int. Conf. Comput., Syst. Signal Process.*, 1984, pp. 1–5.
[6] Y. Ou, E. Hugues-Salas, F. Ntavou, R. Wang, Y. Bi, S. Yan, G. Kanellos, R. Nejabati, and D. Simeonidou, "Field-trial of machine learning-assisted quantum key distribution (QKD) networking with SDN," in *Proc. Eur. Conf. Opt. Commun. (ECOC)*, Sep. 2018, pp. 1–3.
[7] M. Peev, "The SECOQC quantum key distribution network in Vienna," *New J. Phys.*, vol. 11, no. 7, 2009, Art. no. 075001.
[8] G. Vallone, V. D'Ambrosio, A. Sponselli, S. Slussarenko, L. Marrucci, F. Sciarrino, and P. Villoresi, "Free-space quantum key distribution by rotation-invariant twisted photons," *Phys. Rev. Lett.*, vol. 113, no. 6, Aug. 2014, Art. no. 060503.
[9] S.-K. Liao, H.-L. Yong, C. Liu, G.-L. Shentu, D.-D. Li, J. Lin, and H. Dai, "Long-distance free-space quantum key distribution in daylight towards inter-satellite communication," *Nature Photon.*, vol. 11, no. 8, pp. 509–513, Aug. 2017.
[10] S. K. Liao, "Satellite-to-ground quantum key distribution," *Nature*, vol. 549, pp. 43–47, Aug. 2017.
[11] R. Nejabati, R. Wang, A. Bravalheri, A. Muqaddas, N. Uniyal, T. Diallo, R. Tessinari, R. S. Guimaraes, S. Moazzeni, E. Hugues-Salas, G. T. Kanellos, and D. Simeonidou, "First demonstration of quantum-secured, inter-domain 5G service orchestration and on-demand NFV chaining over flexi-WDM optical networks," in *Proc. Opt. Fiber Commun. Conf. Postdeadline Papers*, 2019, pp. 1–3.
[12] *Cerberis3 QKD System*, IDQ, Geneva, Switzerland, 2019.

[13] E. Diamanti, H.-K. Lo, B. Qi, and Z. Yuan, "Practical challenges in quantum key distribution," *NPJ Quantum Inf.*, vol. 2, no. 1, p. 16025, Nov. 2016.
[14] Y. Mao, B.-X. Wang, C. Zhao, G. Wang, R. Wang, H. Wang, F. Zhou, J. Nie, Q. Chen, Y. Zhao, Q. Zhang, J. Zhang, T.-Y. Chen, and J.-W. Pan, "Integrating quantum key distribution with classical communications in backbone fiber network," *Opt. Express*, vol. 26, no. 5, pp. 6010–6020, Mar. 2018.
[15] D. Bacco, L. K. Oxenlowe, A. Zavatta, I. Vagniluca, B. Da Lio, N. Biagi, A. D. Frera, D. Calonico, C. Toninelli, F. S. Cataliotti, and M. Bellini, "Field trial of a finite-key quantum key distribution system in the metropolitan Florence area," in *Proc. Conf. Lasers Electro-Opt. Eur. Eur. Quantum Electron. Conf. (CLEO/Europe-EQEC)*, Jun. 2019, p. 1.
[16] J. F. Dynes, W. W.-S. Tam, A. Plews, B. Fröhlich, A. W. Sharpe, M. Lucamarini, Z. Yuan, C. Radig, A. Straw, T. Edwards, and A. J. Shields, "Ultra-high bandwidth quantum secured data transmission," *Sci. Rep.*, vol. 6, no. 1, p. 35149, Dec. 2016.
[17] L.-J. Wang, K.-H. Zou, W. Sun, Y. Mao, Y.-X. Zhu, H.-L. Yin, Q. Chen, Y. Zhao, F. Zhang, T.-Y. Chen, and J.-W. Pan, "Long-distance copropagation of quantum key distribution and terabit classical optical data channels," *Phys. Rev. A, Gen. Phys.*, vol. 95, no. 1, Jan. 2017, Art. no. 012301.
[18] S. Kleis, J. Steinmayer, R. H. Derksen, and C. G. Schaeffer, "Experimental investigation of heterodyne quantum key distribution in the S-Band embedded in a commercial DWDM system," in *Proc. Opt. Fiber Commun. Conf. (OFC)*, 2019, pp. 1–3, Paper. Th1J.3.
[19] F. Karinou, H. H. Brunner, C.-H.-F. Fung, L. C. Comandar, S. Bettelli, D. Hillerkuss, M. Kuschnerov, S. Mikroulis, D. Wang, C. Xie, M. Peev, and A. Poppe, "Toward the integration of CV quantum key distribution in deployed optical networks," *IEEE Photon. Technol. Lett.*, vol. 30, no. 7, pp. 650–653, Apr. 1, 2018.
[20] R. Kumar, H. Qin, and R. Alléaume, "Coexistence of continuous variable QKD with intense DWDM classical channels," *New J. Phys.*, vol. 17, no. 4, 2015, Art. no. 043027.
[21] P. J. Winzer, "Spatial multiplexing in fiber optics: The 10X scaling of Metro/Core capacities," *Bell Labs Tech. J.*, vol. 19, pp. 22–30, Sep. 2014.
[22] R. S. Luís, B. J. Puttnam, J. M. D. Mendinueta, W. Klaus, J. Sakaguchi, Y. Awaji, T. Kawanishi, A. Kanno, and N. Wada, "OSNR penalty of self-homodyne coherent detection in spatial-division-multiplexing systems," *IEEE Photon. Technol. Lett.*, vol. 26, no. 5, pp. 477–479, Mar. 1, 2014.
[23] X. Pang, "High-speed SDM interconnects with directly-modulated 1.5-μm VCSEL enabled by low-complexity signal processing techniques," in *Proc. Signal Process. Photon. Commun.*, vol. 2018, pp. 1–2, Paper. SpTh2G.4.
[24] J. F. Dynes, S. J. Kindness, S. W.-B. Tam, A. Plews, A. W. Sharpe, M. Lucamarini, B. Fröhlich, Z. L. Yuan, R. V. Penty, and A. J. Shields, "Quantum key distribution over multicore fiber," *Opt. Express*, vol. 24, no. 8, pp. 8081–8087, Apr. 2016.
[25] B. D. Lio, D. Bacco, D. Cozzolino, F. D. Ros, X. Guo, Y. Ding, Y. Sasaki, K. Aikawa, S. Miki, H. Terai, T. Yamashita, J. S. Neergaard-Nielsen, M. Galili, K. Rottwitt, U. L. Andersen, L. K. Oxenlowe, and T. Morioka, "Record-high secret key rate for joint classical and quantum transmission over a 37-core fiber," in *Proc. IEEE Photon. Conf. (IPC)*, Sep. 2018, pp. 10–11.
[26] T. A. Eriksson, B. J. Puttnam, G. Rademacher, R. S. Luís, M. Takeoka, Y. Awaji, M. Sasaki, and N. Wada, "Inter-core crosstalk impact of classical channels on CV-QKD in multicore fiber transmission," in *Proc. Opt. Fiber Commun. Conf. (OFC)*, 2019, pp. 1–3.
[27] G. B. Xavier and G. Lima, "Quantum information processing with space-division multiplexing optical fibres," *Commun. Phys.*, vol. 3, no. 1, p. 9, Dec. 2020.
[28] M. Ureña, I. Gasulla, F. J. Fraile, and J. Capmany, "Modeling optical fiber space division multiplexed quantum key distribution systems," *Opt. Express*, vol. 27, no. 5, pp. 7047–7063, Mar. 2019.
[29] R. Lin, A. Udalcovs, O. Ozolins, X. Pang, L. Gan, L. Shen, M. Tang, S. Fu, S. Popov, C. Yang, W. Tong, D. Liu, T. F. da Silva, G. B. Xavier, and J. Chen, "Telecom compatibility validation of quantum key distribution Co-existing with 112 Gbps/λ/core data transmission in non-trench and trench-assistant multicore fibers," in *Proc. Eur. Conf. Opt. Commun. (ECOC)*, Sep. 2018, pp. 1–3.
[30] B. J. Puttnam, R. S. Luís, G. Rademacher, A. Alfredsson, W. Klaus, J. Sakaguchi, Y. Awaji, E. Agrell, and N. Wada, "Characteristics of homogeneous multi-core fibers for SDM transmission," *APL Photon.*, vol. 4, no. 2, Feb. 2019, Art. no. 022804.
[31] E. Agrell, "Roadmap of optical communications," *J. Opt.*, vol. 18, no. 6, 2016, Art. no. 063002.
[32] X. Ma, B. Qi, Y. Zhao, and H.-K. Lo, "Practical decoy state for quantum key distribution," *Phys. Rev. A, Gen. Phys.*, vol. 72, no. 1, 2005, Art. no. 012326.
[33] C. Gobby, Z. L. Yuan, and A. J. Shields, "Quantum key distribution over 122 km of standard telecom fiber," *Appl. Phys. Lett.*, vol. 84, no. 19, pp. 3762–3764, May 2004.
[34] P. Eraerds, N. Walenta, M. Legré, N. Gisin, and H. Zbinden, "Quantum key distribution and 1 gbps data encryption over a single fibre," *New J. Phys.*, vol. 12, no. 6, 2010, Art. no. 063027.
[35] T. Ferreira da Silva, G. B. Xavier, G. P. Temporao, and J. P. von der Weid, "Impact of Raman scattered noise from multiple telecom channels on fiber-optic quantum key distribution systems," *J. Lightw. Technol.*, vol. 32, no. 13, pp. 2332–2339, Jul. 1, 2014.
[36] *WaveShaper Series A Family of Programmable Optical Processors*, Finisar, Sunnyvale, CA, USA, 2019.
[37] N. Lütkenhaus, "Estimates for practical quantum cryptography," *Phys. Rev. A, Gen. Phys.*, vol. 59, no. 5, pp. 3301–3319, May 1999.
[38] W.-H. Jiang, J.-H. Liu, Y. Liu, G. Jin, J. Zhang, and J.-W. Pan, "1.25 GHz sine wave gating InGaAs/InP single-photon detector with a monolithically integrated readout circuit," *Opt. Lett.*, vol. 42, no. 24, pp. 5090–5093, Dec. 2017.

RUI LIN (Member, IEEE) received the bachelor's degree in electrical and information engineering from the Huazhong University of Science and Technology (HUST), Wuhan, China, in 2011, and the Ph.D. degree in communication system from the KTH Royal Institute of Technology, Stockholm, Sweden, in 2016. She is currently working as a Postdoctoral Researcher with the Department of Electrical Engineering, Chalmers University of Technology, Gothenburg, Sweden. Her research interests include enabling technologies for high-speed optical communication networks and cyber security.

ALEKSEJS UDALCOVS (Member, IEEE) received the M.Sc. degree in telecommunications and the Doctor of Engineering Science (Dr.Sc.Ing.) degree in electronics and telecommunications from Riga Technical University, Riga, Latvia, in 2011 and 2015, respectively. From 2012 to 2016, he was a Visiting Ph.D. Researcher within the Swedish Institute Visby programme and then a Postdoctoral Researcher within the EU project GRIFFON, KTH Royal Institute of Technology, Stockholm, Sweden. In mid-2015, he also joined KTH/RISE Kista High Speed Transmission Lab, and later he moved to RISE Research Institutes of Sweden after receiving the research grant named SCENE—Spectrum, cost, and energy trade-offs in optical networks from the Swedish ICT TNG consortium. Since 2019, he has been a Senior Scientist with RISE, who is working in cooperation with industry and academia providing his expertise in communication technologies. He is a (co)author of more than 100 articles in peer-reviewed international journals and conferences. Furthermore, he has participated in numerous experimental activities in a number of research groups (in Sweden—KTH, RISE; in Germany—VPIphotonics GmbH; in Belgium—Ghent University; in France—III–V Lab; in Denmark—DTU Fotonik) on fiber-optic transmission experiments, modeling of fiber-optic links and (sub-) systems, and optical network planning. His main research interests are within the PHY-layer aspects in optical transport and photonic-wireless networks.

OSKARS OZOLINS (Member, IEEE) received the M.Sc. degree in telecommunications and the Dr.Sc.Ing. (Ph.D.) degree in optical communications from Riga Technical University, Riga, Latvia, in 2009 and 2013, respectively. He is currently a Senior Scientist and Technical Lead with the Kista High-speed Transmission Lab (Kista HST-Lab), RISE Research Institutes of Sweden (former ACREO) under Swedish Research Council starting grant project Photonic-assisted signal processing techniques (PHASE). He is also appointed as an Affiliated Faculty on Optical Communication at the Department of Applied Physics, KTH Royal institute of Technology. His research interests are in the areas of digital and photonic-assisted signal processing techniques, high-speed short-reach communications and devices, optical and photonic-wireless interconnects, and single photon quantum communication. He is the author of around 170 international journal publications, conference contributions, invited talks, patents and book chapters. He has regularly served as a Designated Reviewer for the IEEE/OSA Journals: *Chinese Optics Letters*, *Applied Optics*, *Optics Express*, *Photonics Technology Letters*, the *Journal of Lightwave Technology* and *Photonics Research*.

XIAODAN PANG (Senior Member, IEEE) received the M.Sc. degree in photonics from the KTH Royal Institute of Technology, Stockholm, Sweden, in 2010, and the Ph.D. degree in optical communications from the DTU Fotonik, Technical University of Denmark, in 2013. His research interests include fiber-optic communications, short-reach optical interconnects, terahertz photonics and free-space optics. Dr. Pang is the coordinator of the EU H2020 Marie Curie Individual Fellowship Project NEWMAN (2018–2020). He was a TPC Member of the Asia Communications and Photonics Conference (ACP'2018–2019) and is a member of the Digital subsystems and systems for data centers subcommittee for the 43rd Optical Networking and Communication Conference (OFC'2020).

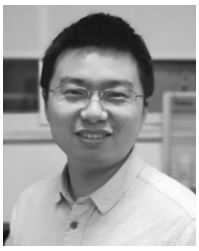

LIN GAN was born in Hubei, China, in 1993. He received the B.S. degree in optical information science and technology from the Huazhong University of Science and Technology (HUST), China, in 2015, where he is currently pursuing the Ph.D. degree with the Next Generation Internet Access System National Engineering Lab. His research interests include space division multiplexing transmission and fiber sensing.

MING TANG (Senior Member, IEEE) received the B.Eng. degree from the Huazhong University of Science and Technology (HUST), Wuhan, China, in 2001, and the Ph.D. degree from Nanyang Technological University (NTU), Singapore, in 2006. He conducted the Postdoctoral Research Fellowship in the Network Technology Research Centre (NTRC), NTU from 2006 to 2009, focusing on the optical fiber amplifier, high-power fiber lasers, nonlinear fiber optics, and all-fiber signal processing. From February 2009 to 2011, he was a Research Scientist with Tera-Photonics Group, led by Prof. H. Ito in RIKEN, Sendai, Japan, conducting research on terahertz-wave generation, detection, and application using nonlinear optical technologies. Since March 2011, he has been a Professor with the School of Optical and Electronic Information, Wuhan National Laboratory for Optoelectronics, HUST. He has published more than 200 technical articles in the international recognized journals and conferences (cited more than 2500 times in Google Scholar, H-index 24). His current research is concerned with the high-speed optical fiber communications, including the novel transmission fibers and the advanced digital signal processing techniques. He has been a member of the IEEE Photonics Society since 2001, and also a member of the Optical Society of America. He has been awarded the NSFC Excellent Young Scholar, and the new century talent program of MOE in China.

SONGNIAN FU (Senior Member, IEEE) has been a Professor with the School of Optical and Electronic Information and the Wuhan National Laboratory for Optoelectronics, Huazhong University of Science and Technology, Wuhan, China, since February 2011. His research interests include fiber optics and fiber optical transmission.

SERGEI POPOV received the M.Sc. degree in applied physics and the M.Sc. degree in computer science, Russia, in 1987 and 1989, respectively, and the Ph.D. degree in applied physics, Finland, in 1991. He is currently a Professor with the Applied Physics Department, Royal Intitute of Technology (KTH), Stockholm, Sweden. He stayed with Ericsson Telecom AB and Acreo AB (both in Sweden) before joining KTH. His expertise is in optical communication, laser physics, plasmonics, and optical materials. He (co)authored over 300 articles and conference contribution. He is an OSA Fellow, and the Editor-in-Chief of JEOS: RP journal (EOS).

THIAGO FERREIRA DA SILVA received the B.Sc. degree in telecommunications engineering from the Catholic University of Petrópolis, Petrópolis, Brazil, in 2005, and the M.Sc. and D.Sc. degrees in electrical engineering from the Pontifical Catholic University of Rio de Janeiro, Rio de Janeiro, Brazil, in 2008 and 2011, respectively. Since 2008, he has been a Researcher with the Optical Metrology Division, National Institute of Metrology, Quality and Technology, Brazil. His research interests include single-photon detectors, fiber-optic quantum communications, and optical metrology.

GUILHERME B. XAVIER received the Ph.D. degree in electrical engineering from the Pontifical Catholic University of Rio de Janeiro, Rio de Janeiro, Brazil, in 2009. He held an Associate Professor post at the University of Concepción in Chile until 2017. He is currently an Associate Professor with the Department of Electrical Engineering, Linköping University, Sweden. His research interests are experimental quantum communications through optical fibers, integration of quantum information processing technologies with current telecommunication systems, and fundamental experiments in quantum optics. He has coordinated several research grants in the field of quantum communications and published over 40 articles in peer-reviewed top journals in Physics and Optics.

JIAJIA CHEN (Senior Member, IEEE) received the bachelor's degree from Zhejiang University, China, in 2004, and the Ph.D. degree from the KTH Royal Institute of Technology, Sweden, in 2009. She is currently a Professor with the Chalmers University of Technology, Sweden. She and her group have made advances in optical network architecture design along with the supporting transmission techniques and resource allocation strategies, which greatly improve capacity, reliability, energy efficiency and cost efficiency in access, core, and data center networks. She has been sharing her knowledge with the technical community with many peer-reviewed journal articles, conference papers, invited talks (more than 200 publications to-date), and ten patent applications. She has been organizing several IEEE international conferences in the field and serving on technical program committees, including OFC (Subcommittee Chair 2019), ECOC, Globecom (Symposium Co-Chair 2020), ICC, and so on.